HHS Public Access

Author manuscript

*Mol Microbiol*. Author manuscript; available in PMC 2015 April 25.

Published in final edited form as:

*Mol Microbiol*. 2009 August ; 73(4): 622–638. doi:10.1111/j.1365-2958.2009.06795.x.

# Genetic and Biochemical Analyses of the *Pseudomonas aeruginosa* Psl Exopolysaccharide Reveal Overlapping Roles for Polysaccharide Synthesis Enzymes in Psl and LPS Production

**Matthew S. Byrd**[1], **Irina Sadovskaya**[2], **Evgueny Vinogradov**[3], **Haiping Lu**[1], **April B. Sprinkle**[1], **Stephen H. Richardson**[1], **Luyan Ma**[4], **Brad Ralston**[1], **Matthew R. Parsek**[5], **Erin M. Anderson**[6], **Joseph S. Lam**[6], and **Daniel J. Wozniak**[4,*]

[1]Department of Microbiology and Immunology, Wake Forest University School of Medicine, Winston-Salem, NC 27157

[2]Laboratoire de Recherche sur les Biomatériaux et les Biotechnologies IFR 114, Université du Littoral-Côte d'Opale, Bassin Napoléon, BP 120, 62327 Boulogne-sur-mer, France

[3]Institute for Biological Sciences, National Research Council of Canada, 100 Sussex Drive, Ottawa, ON, Canada KIAOR6

[4]Center for Microbial Interface Biology, The Ohio State University, Columbus, Ohio 43210

[5]Department of Microbiology, University of Washington, Seattle, WA

[6]Department of Molecular and Cellular Biology, University of Guelph, Guelph, Ontario, Canada

## Abstract

Exopolysaccharides contribute significantly to attachment and biofilm formation in the opportunisitc pathogen *Pseudomonas aeruginosa*. The Psl polysaccharide, which is synthesized by the *p*olysaccharide *s*ynthesis *l*ocus (*psl*), is required for biofilm formation in nonmucoid strains that do not rely on alginate as the principal biofilm polysaccharide. In-frame deletion and complementation studies of individual *psl* genes revealed that eleven *psl* genes, *pslACDEFGHIJKL*, are required for Psl production and surface attachment. We also present the first structural analysis of the *psl*-dependent polysaccharide, which consists of a repeating pentasaccharide containing D-mannose, D-glucose, and L-rhamnose:

$$[\rightarrow 3)-\beta-\mathrm{D}-\underset{\alpha-\mathrm{D}-\mathrm{Man}p}{\overset{\mathrm{Man}p}{\overset{2}{\uparrow}\\1}}-(1\rightarrow 3)-\beta-\mathrm{D}-\mathrm{Man}p-(1\rightarrow 3)-\alpha-\mathrm{L}-\mathrm{Rha}p-(1\rightarrow 3)-\beta-\mathrm{D}-\mathrm{Glc}p-(1\rightarrow]_{\mathrm{n}-}$$

In addition we identified the sugar nucleotide precursors involved in Psl generation and demonstrated the requirement for GDP-D-mannose, UDP-D-glucose, and dTDP-L-rhamnose in Psl

*Corresponding author: Daniel J. Wozniak, Division Infectious Disease, Microbiology, Center for Microbial Interface Biology, The Ohio State University, 1018 Biomedical Research Tower, 460 W 12th Ave., Columbus OH 3210 Daniel.wozniak@osumc.edu.

production and surface attachment. Finally, genetic analyses revealed that *wbpW* restored Psl production in a *pslB* mutant and *pslB* promoted A-band LPS synthesis in a *wbpW* mutant, indicating functional redundancy and overlapping roles for these two enzymes. The structural and genetic data presented here provide a basis for further investigation of the Psl proteins and potential roles for Psl in the biology and pathogenesis of *P. aeruginosa*.

## Introduction

*Pseudomonas aeruginosa* is a Gram-negative pathogen responsible for a variety of opportunistic infections, including chronic airway infections in patients with cystic fibrosis (CF) (Driscoll *et al.*, 2007; Govan and Deretic, 1996). During the course of chronic infection, *P. aeruginosa* forms matrix-encased, surface-associated communities called biofilms. Biofilms are thought to contribute to persistence in the CF airway by contributing to evasion of the host immune response and antimicrobial therapy (Parsek and Singh, 2003; Ramsey and Wozniak, 2005; Stewart and Costerton, 2001). Polysaccharide has been identified as a significant component of the *P. aeruginosa* biofilm matrix (Branda *et al.*, 2005) with alginate, an unbranched heteropolymer of β-1,4-linked D-mannuronic and D-guluronic acids, as the defining polysaccharide of clinical mucoid isolates (Govan and Deretic, 1996; Ramsey and Wozniak, 2005). Nonmucoid *P. aeruginosa* strains do not rely on alginate for production of the biofilm matrix, but instead utilize the exopolysaccharides Pel and/or Psl (Branda *et al.*, 2005; Ryder *et al.*, 2007; Wozniak *et al.*, 2003). The *pel* locus contains seven genes involved in the production of a glucose-rich polysaccharide important in pellicle formation in standing liquid cultures and maintenance of biofilm structure (Friedman and Kolter, 2004a; Vasseur *et al.*, 2005). The *p*olysaccharide *s*ynthesis *l*ocus (*psl*) is a group of fifteen co-transcribed genes proposed to encode the necessary enzymes for Psl biosynthesis (Friedman and Kolter, 2004b; Jackson *et al.*, 2004; Matsukawa and Greenberg, 2004). It is predicted by us and others that the resulting polysaccharide contains D-mannose (D-Man), D-glucose (D-Glc), and L-rhamnose (L-Rha), and possibly galactose, although the structure of this key biofilm matrix component is unknown (Friedman and Kolter, 2004b; Jackson *et al.*, 2004; Ma *et al.*, 2007; Matsukawa and Greenberg, 2004; Rocchetta *et al.*, 1998; Wozniak *et al.*, 2003).

*P. aeruginosa* has the potential to produce several polysaccharides or polysaccharide-containing compounds. Besides alginate, Pel, and Psl, *P. aeruginosa* can make two other important polysaccharide-containing compounds, rhamnolipid and lipopolysaccharide (LPS). Although their structures are radically different, two or more of these compounds shares some of the same basic building blocks. Polysaccharide synthesis commonly relies on a pool of sugar nucleotide precursors which are modified or directly incorporated into the elongating polysaccharide chain (Rocchetta *et al.*, 1999; Samuel and Reeves, 2003; Whitfield and Roberts, 1999). In addition to the proposed composition of Psl, one or more of the sugar nucleotide precursors GDP-D-Man, UDP-D-Glc, and dTDP-L-Rha is also critical for the production of alginate, rhamnolipid, both types of *P. aeruginosa* LPS, and potentially Pel. AlgD uses GDP-D-Man as a substrate for the first step in alginate biosynthesis (Govan and Deretic, 1996; Ramsey and Wozniak, 2005). Rhamnolipid synthesis requires dTDP-L-Rha, which is linked by a β-glycosidic bond to a 3-hydroxyfatty acid in mono- or di-

rhamnose configurations (Soberon-Chavez *et al.*, 2005). A-band LPS is a homopolymer of α-1,2, α-1,3, α-1,3-linked D-Rha trisaccharides attached to core oligosaccharide-lipid A (Rivera *et al.*, 1988; Rivera and McGroarty, 1989; Rocchetta *et al.*, 1998). B-band LPS is a serotype-specific heteropolymer. The common laboratory wild-type strain, PAO1, belongs to serotype O5, and produces B-band LPS containing an O-antigen trisaccharide repeating unit of 2-acetamido-3-acetamidino-2,3-dideoxy-D-mannuronic acid [Man(2NAc3N)A], 2,3-diacetamido-D-mannuronic acid [Man$(NAc)_2$A], and 2-acetamido-2,6-dideoxy-D-galactose (Fuc2NAc) (Rocchetta *et al.*, 1998; Rocchetta *et al.*, 1999). Synthesis of A-band LPS relies on GDP-D-Man as a precursor to D-Rha (Rocchetta *et al.*, 1998), and both A-band and B-band LPS require dTDP-L-Rha as L-Rha is the linking sugar for B-band and presumably A-band attachment to the outer core. Although B-band LPS is typically reduced in *P. aeruginosa* CF isolates, nonmucoid PAO1 expresses both A-band and B-band LPS (Hancock *et al.*, 1983; Rocchetta *et al.*, 1999).

In this study we show that eleven of the fifteen *psl* genes are necessary for Psl synthesis, while four *psl* genes, *pslB*, *pslM*, *pslN*, and *pslO*, are not required. Prior to this study there had been no structural investigation of the Psl polysaccharide. Using an inducible Psl overexpression strain to generate polysaccharide, we determined that a fraction of Psl is released from the cell in the form of a branched pentasaccharide repeating unit containing D-Man, D-Glc, and L-Rha. This was predicted by prior analyses (Friedman and Kolter, 2004b; Jackson *et al.*, 2004; Kocharova *et al.*, 1988; Matsukawa and Greenberg, 2004; Rocchetta *et al.*, 1998; Wozniak *et al.*, 2003) and is identical to that described previously by Kocharova *et al.* (1988). We inactivated one or more critical genes in each sugar nucleotide precursor pathway and show that GDP-D-Man, UDP-D-Glc, and dTDP-L-Rha are each required for Psl production. We also discovered that the A-band LPS gene product, WbpW, functions in the synthesis of both Psl and A-band LPS.

## Results and Discussion

### Anti-Psl antiserum specifically detects Psl

To assist in detecting Psl in polysaccharide extracts, we had antiserum (α-Psl) generated to the extracellular material from the arabinose-inducible Psl overexpression strain WFPA801 (Ma *et al.*, 2006). The antiserum was then adsorbed multiple times against WFPA800, a strain engineered that lacks Psl due to a deletion in the promoter region upstream of *pslA* (Ma *et al.*, 2006). The specificity of α-Psl was first determined by immunoblotting polysaccharide extracts from wild type and three *psl* mutants. The *psl* operon structures of these four strains are shown in Fig. 1A, along with the putative functions of *psl*-encoded gene products as annotated previously (Friedman and Kolter, 2004b; Jackson *et al.*, 2004; Stover *et al.*, 2000). WFPA826 contains a deletion from upstream of *pslA* to downstream of *pslO*, removing all *psl* open reading frames. As shown in Fig. 1B, when immunoblotted, extracts from these strains revealed the predicted interactions with the α-Psl antiserum. Extracts from WFPA800 and WFPA826 did not react with α-Psl, while WFPA801 extracts reacted strongly with α-Psl, requiring a 1:50 dilution to be within the range of chemiluminescent detection. The fact that WFPA800 has the same loss of α-Psl reactivity as WFPA826 confirms that the *psl* promoter deletion is a valid negative control for Psl

synthesis. The intermediate reactivity of PAO1 extracts with α-Psl demonstrates a lower level of Psl being produced by the wild type strain as compared to the level produced by induced strain WFPA801.

## Mutagenesis reveals that all *psl* genes except *pslBMNO* are necessary for Psl synthesis and *P. aeruginosa* attachment

When initially studied, the *psl* locus was found to encode fifteen co-transcribed open reading frames predicted to be involved in polysaccharide synthesis (Friedman and Kolter, 2004b; Jackson *et al.*, 2004; Matsukawa and Greenberg, 2004). The phenotype of a *psl* promoter deletion mutant is a severe attenuation of surface attachment and biofilm forming ability under both static and continuous flow conditions (Ma *et al.*, 2006). Few studies have been carried out on deletion mutants of individual *psl* genes (Campisano *et al.*, 2006; Friedman and Kolter, 2004b; Jackson *et al.*, 2004; Ma *et al.*, 2007), but of those, all show essential roles in biofilm formation. To investigate the contribution of each *psl* gene to generation of Psl and the attachment phenotype, in-frame, non-polar deletions were made in each *psl* gene following a similar overlapping PCR strategy to that which was used to create WFPA800 (Table 1) (Ma *et al.*, 2006). The ability of these fifteen mutants to attach to a solid surface was first assessed by crystal violet staining (Fig. 2A), with values normalized to the PAO1 background strain. Attachment of WFPA800 and eleven *psl* mutants (*pslACDEFGHIJKL*) was significantly reduced ($p<0.001$, Dunnett's Test following one-way ANOVA) compared to that of PAO1. Interestingly, deletion of *pslB*, *pslM*, *pslN*, or *pslO* did not result in an observable attachment defect compared to PAO1. Polysaccharide extracts from each of the *psl* mutants were blotted on nitrocellulose and probed with α-Psl to directly evaluate Psl production (Fig. 2A). The same eleven strains that were deficient in attachment likewise did not produce detectable levels of Psl. Mutants that had comparable attachment to PAO1, however, did produce Psl. The correlation between Psl production and solid surface attachment has been previously reported (Friedman and Kolter, 2004b; Jackson *et al.*, 2004; Ma *et al.*, 2006; Ma *et al.*, 2007; Ma *et al.*, 2009), and this analysis of individual *psl* mutants confirms these observations.

We were able to quantify Psl production by individual *psl* mutants using an ELISA assay, in which Psl-specific antiserum was used to detect Psl in polysaccharide extracts bound to 96-well microtiter plates. A standard curve using purified Psl allowed us to quantify the amount of Psl (Fig. 2B). Similar to both the crystal violet staining and immunoblot, the ELISA revealed that eleven *psl* genes, *pslACDEFGHIJKL*, are essential for Psl production. The differences in Psl produced by these eleven Psl-deficient mutants were highly significant by Dunnett's Test ($p<0.001$) compared to PAO1. When complemented by plasmids expressing the relevant *psl* gene, each of these mutants produced Psl at levels comparable to or greater than wild type (data not shown). This provides convincing genetic evidence that most but not all of the *psl* genes within the operon are required for Psl synthesis and the attachment phenotype linked to Psl.

The lack of an attachment phenotype or effect on Psl production in *pslM*, *pslN*, and *pslO* mutants (*pslB* is discussed below) does not exclude these genes as members of the *psl* operon. However, recent transcriptional profiling data reveals that *pslM*, *pslN*, and *pslO* are

not co-transcribed with *pslA-pslL* (Goodman *et al.*, 2004; Hickman *et al.*, 2005; Starkey *et al.*, 2009). It is conceivable that these three gene products may have regulatory functions in the Psl pathway, or might modify the polysaccharide without altering its attachment properties or epitopes recognized by α-Psl. Further work will need to be done to determine the inclusion and precise function of the last three genes in the *psl* operon.

## Psl is a pentasaccharide containing D-Man, D-Glc, and L-Rha

As no polysaccharide structure has been definitively associated with the *psl* locus, we first sought to determine Psl structure using biochemical approaches. *P. aeruginosa* WFPA801 cells were grown statically in a chemically defined medium (Vasseur *et al.*, 2007) supplemented with arabinose (0.4% final concentration) in order to induce the production of Psl. Upon growth, the bacteria produced thick transparent extracellular material, composed mostly of nucleic acids and proteins, which is in good agreement with literature data (Matsukawa and Greenberg, 2004). Crude carbohydrate extracts were obtained from both cell-associated matrix and from the growth medium, then further treated to remove nucleic acids and proteins. These methods of purification of carbohydrate polymers, as described in the Experimental Procedures, have been previously employed for the isolation of extracellular teichoic acids from staphylococcal biofilms (Sadovskaya *et al.*, 2004; Vinogradov *et al.*, 2006).

The total carbohydrate extract was fractionated on a Sephadex G-50 column. A typical elution profile of the crude carbohydrate of the growth medium (1 L) is shown in Fig. 3A. Fractionation of the carbohydrate extract of the cell-surface-associated matrix gave similar profiles (data not shown). The majority of carbohydrate material eluted in lower MW fractions, in the range of 3000-6000. Yields of this material reached 10 mg/L of culture from the growth medium, while an additional 2-3 mg was obtained from the cell-associated matrix. The material was separated in three fractions, A, B, and C, according to the MW (Fig. 3A). Monosaccharide analysis of fraction C indicated the presence of Man, Glc, and Rha in the approximate ratios of 3:1:1. Monosaccharide analysis and NMR spectra of fraction B indicated a complex mixture, containing β-(1,3)-linked glycerophosphorylated glucan and LPS, but also Man, Glc, and Rha (Vinogradov *et al.*, unpublished data). Polysaccharide from fraction C was chosen for the detailed NMR analysis due to better quality of its NMR spectra. Its structure was analyzed by 2D NMR spectroscopy, and was found to have a pentasaccharide repeating unit structure I (Table 2 and Fig. 4).

$$[\rightarrow 3)-\beta-\mathrm{D}-\underset{\substack{\uparrow\\ 1\\ \alpha-\mathrm{D}-\mathrm{Man}p\\ \mathrm{A}}}{\overset{\substack{\mathrm{C}\\ \mathrm{Man}p\\ 2}}{}}-(1\rightarrow 3)-\beta-\mathrm{D}-\overset{\mathrm{D}}{\mathrm{Man}p}-(1\rightarrow 3)-\alpha-\mathrm{L}-\overset{\mathrm{B}}{\mathrm{Rha}p}-(1\rightarrow 3)-\beta-\mathrm{D}-\overset{\mathrm{E}}{\mathrm{Glc}p}-(1\rightarrow]_{\mathrm{n}-} \quad \mathrm{I}$$

The structure of this repeating unit is identical to the one of the low molecular weight neutral extracellular polysaccharide of a clinical isolate of *P. aeruginosa* immunotype 4 and has been characterized earlier (Kocharova *et al.*, 1988).

In addition to the monosaccharides of the polymeric chain, signals of the reducing terminal α- and β-Glc, substituted by variants of α-Rha were present. Signals of the residue C, not substituted at O-3 by Glc E, (C′) were also identified (Table 2), thus indicating the presence of a pentasaccharide, corresponding to a single repeating unit with the Glc residue E at the reducing end (II):

$$\alpha\text{-D-}\overset{A'}{\text{Man}}p\text{-}(1\rightarrow 2)\text{-}\beta\text{-D-}\overset{C'}{\text{Man}}p\text{-}(1\rightarrow 3)\text{-}\beta\text{-D-}\overset{D}{\text{Man}}p\text{-}(1\rightarrow 3)\text{-}\alpha\text{-L-}\overset{B}{\text{Rha}}p\text{-}(1\rightarrow 3)\text{-}\overset{\alpha\text{-E}',\beta\text{-E}''}{\text{D-Glc}}p \quad \text{II}$$

Integration of the H/C-2 signals of the residues B, C, D (Fig. 4) shows that the overall degree of polymerization is very small, and the mixture may contain an equimolar amount of components with n = 1, 2, and 3, with very little amount of longer chains.

In agreement with the NMR data, methylation analysis of the polysaccharides of fractions B and C indicated the presence of terminal Man*p*, 3-*O*-substituted Man*p*, 2,3-*O*-substituted Man*p*, 3-*O*-substituted Glc*p* and 3-*O*-substituted Rha*p*; as well as 2-*O*-substituted Man*p* characteristic for structure II. Methylation analysis indicated an average length of 1-2 repeating units in polysaccharide from fraction C and 4-5 repeating units in polysaccharide from fraction B.

Wild type *P. aeruginosa* PAO1 were grown in identical conditions but without the addition of arabinose, and the crude polysaccharide extract was fractionated on a Sephadex G-50 column. A low MW polysaccharide containing Man, Glc, and Rha eluted at ∼4000. In a separate experiment, we assessed relative quantities of the Man-containing polysaccharide in the wild type and WFPA801 strains and found it to be ∼4 times higher in the WFPA801 strain with Psl synthesis induced with 0.4% arabinose (data not shown), which is in a good agreement with the transcription data (Ma *et al.*, 2006).

Importantly, no Man-containing carbohydrates were detected in the cell-associated matrix or growth media of the *psl* promoter deletion mutant WFPA800 (data not shown). From these analyses we can affirm that a Man-rich polysaccharide is indeed the product of the *psl* locus. The chemical structure of the repeating unit of this polysaccharide has been determined and was found to be identical to one described in the literature (Kocharova *et al.*, 1988). We have found that the polysaccharides produced by the *psl*-inducible strain WFPA801 and the wild-type strain PAO1 had a slightly lower average MW than the polysaccharide described by Kocharova *et al.* In addition, we were able to identify a biological repeating unit of this polysaccharide (Structure II).

To determine α-Psl antiserum reactivity with fractionated polysaccharide, WFPA800 and WFPA801 cells were grown in LBNS supplemented with 2% L-arabinose, then treated with ethanol/$CaCl_2$ and proteinase K as described in Experimental Procedures. The crude cell-associated polysaccharide was fractionated on a Sephadex G-50 column (Fig. 3B) and three fractions corresponding to fractions A-C in Fig. 3A were evaluated for Psl by immunoblot analysis. The high MW fraction from WFPA801 reacted strongly with α-Psl, while the two low MW fractions did not show detectable reactivity with the antiserum (Fig. 3C). The monosaccharide composition of this high MW fraction is consistent with the structure of Psl

(data not shown). The lack of reactivity with either low MW fraction is currently under investigation. However, high MW cell-associated polysaccharide of WFPA800 did not react with α-Psl, confirming that the α-Psl antiserum is Psl-specific but is likely directed primarily towards a high MW form of Psl (Fig. 3C). Quantities of low MW cell-associated polysaccharide from WFPA800 sufficient for immunoblotting could not be obtained.

A study performed over two decades ago identified a neutral, low molecular weight (~6500) polysaccharide with a pentasaccharide repeating unit in a clinical *P. aeruginosa* isolate. The pentasaccharide repeating unit consisted of D-Glc, D-Man, and L-Rha:

$$-3)-\beta-\mathrm{D}-\mathrm{Glc}p-(1-3)-\beta-\mathrm{D}-\underset{\substack{2\\1\\\alpha-\mathrm{D}-\mathrm{Man}p}}{\mathrm{Man}p}-(1-3)-\beta-\mathrm{D}-\mathrm{Man}p-(1-3)-\alpha-\mathrm{L}-\mathrm{Rha}p-(1-$$

Antibodies to this pentasaccharide were cross-reactive with LPS from several Fisher immunotype strains of *P. aeruginosa*, suggesting that the structure may be a conserved component of the LPS core or O-antigen (Kocharova *et al.*, 1988). However, the large proportion of D-Man in this structure is not consistent with the lack of such residues in the inner core or either of the two outer core glycoforms (Bystrova *et al.*, 2006; Komarova *et al.*, 2008; Poon *et al.*, 2008). Additionally, no structures identical or highly similar to this pentasaccharide have been reported in *P. aeruginosa* O-antigen polysaccharides to date (Rocchetta *et al.*, 1999). A later study investigating the synthesis of the A-band LPS precursor D-Rha identified a cluster of three open reading frames predicted to encode enzymes involved in production of a polysaccharide containing D-Man, D-Glc, and L-Rha (Rocchetta *et al.*, 1998). The authors speculated that the gene cluster which they identified might be responsible for a polysaccharide distinct from LPS and alginate, and could account for the pentasaccharide repeating unit published by Kocharova *et al.* (Rocchetta *et al.*, 1998). Following the publication of the *psl* locus by three individual groups (Friedman and Kolter, 2004b; Jackson *et al.*, 2004; Matsukawa and Greenberg, 2004), it was clear that the three ORFs found by Rocchetta *et al.* were the first three genes in the *psl* cluster, *pslA*, *pslB*, and *pslC*. This observation raised the hypothesis that the newly annotated *psl* locus encoded enzymes necessary for constructing the polysaccharide isolated by Kocharova *et al.*, but the hypothesis was not followed up until this investigation of the structure of Psl polysaccharide.

Previous reports are conflicting as to the presence of galactose in Psl (Friedman and Kolter, 2004b; Ma *et al.*, 2007; Matsukawa and Greenberg, 2004; Wozniak *et al.*, 2003). Binding of a galactose-specific lectin to intact *P. aeruginosa* was shown to be *psl*-dependent, and monosaccharide analysis revealed galactose and mannose as predominant extracellular components of WFPA801 induced with 2% arabinose (Ma *et al.*, 2007). However, we did not detect significant levels of galactose in any carbohydrate preparation used for structural or antiserum reactivity experiments. In the present study, NMR was utilized as a more accurate and direct method of structural determination compared with lectin binding assays and compositional analyses used previously. It is also possible that variations in growth

conditions used in these studies could account for the differences in monosaccharide composition.

### Shared sugar nucleotide precursors involved in Psl synthesis

Knowing the structure of Psl allowed us to then identify the pathways involved in production of precursor sugars used by Psl enzymes, and determine if Psl production is affected when these pathways are disturbed. The pathways and the Psl structure indicating the proposed location of incorporated sugars are summarized in Fig. 5. The sugar nucleotide precursors GDP-D-Man, UDP-D-Glc, and dTDP-L-Rha are synthesized in three distinct pathways, making removal of one sugar at a time possible (Rahim *et al.*, 2000; Rocchetta *et al.*, 1998; Rocchetta *et al.*, 1999). It is important to note that while the biosynthetic gene clusters for the previously mentioned *P. aeruginosa* polysaccharides are located at sites distinct from the *psl* locus (Friedman and Kolter, 2004b; Jackson *et al.*, 2004; Matsukawa and Greenberg, 2004), the use of common precursors, as discussed in the introduction, suggests functional overlap of known polysaccharide synthesis enzymes with gene products of the *psl* locus.

### dTDP-L-Rha is necessary for Psl synthesis

Consistent with the presence of L-Rha in the Psl structure (I), and to provide an independent validation of the Psl structure, we reasoned that disrupting the L-Rha pathway would result in a loss of Psl synthesis and a defect in surface attachment. The *rml* locus is responsible for the generation of dTDP-L-Rha, the sugar-nucleotide precursor allowing L-Rha to be incorporated in the LPS outer core and rhamnolipid, as well as the O polysaccharide of certain *P. aeruginosa* serotypes (Rahim *et al.*, 2000). RmlC is a dTDP-4-keto-6-deoxy-D-glucose-3,5-epimerase that catalyzes the penultimate step in the dTDP-L-Rha pathway, and when deleted, results in a defect in LPS outer core synthesis leading to a loss of both A-band polysaccharide and B-band O-antigen on the cell surface (Dong *et al.*, 2007; Rahim *et al.*, 2000). The O-antigen defect in an *rmlC* mutant is in agreement with results obtained by previous studies demonstrating that L-Rha is the acceptor residue for O-antigen addition to the outer core (Sadovskaya *et al.*, 1998; Sadovskaya *et al.*, 2000). It is likely that terminal L-Rha on the outer core is also the site of attachment for A-band polysaccharide, but this has not been definitively established (Rahim *et al.*, 2000) and work is underway by two of the authors, Lam and Vinogradov, to address this issue.

An *rmlC* mutant was evaluated for surface attachment and Psl production by immunoblot (Fig. 6). There was a significant decrease in the attachment of the *rmlC* mutant compared to the parental wild type PAO1 strain in which this mutation was generated ($p<0.001$, Dunnett's Test), but not as severe a defect as in WFPA800 (Δpr, Fig. 6). Immunoblotting polysaccharide extract from the *rmlC* mutant with α-Psl antiserum did not reveal any detectable Psl, implicating the *rml* locus in its production by providing the L-Rha precursor dTDP-L-Rha. The fact that the *rmlC* mutant shows greater attachment than WFPA800 might be attributed to the altered surface physiology of the *rmlC* mutant compared to WFPA800, due to a loss of both A-band polysaccharide and B-band O-antigen from the cell surface. Previous reports have indicated an increase in surface adherence in certain *P. aeruginosa*

strains lacking both A-band and B-band LPS, but this has not been confirmed for all serotypes (Rocchetta *et al.*, 1999).

To determine if the attachment defect in the *rmlC* mutant might be due to effects on LPS, a *waaL* mutant was examined (Fig. 6). WaaL is the O-antigen ligase responsible for addition of both A-band polysaccharide and B-band O-antigen to the LPS core (Abeyrathne and Lam, 2007). The LPS phenotypes of *rmlC* and *waaL* mutants are similar in that A- and B-band polysaccharides are not displayed on the cell surface but instead remain linked to the lipid carrier undecaprenol-phosphate (Und-P) (Abeyrathne *et al.*, 2005; Rahim *et al.*, 2000). Interestingly, attachment of the *waaL* mutant was significantly greater than that of PAO1 ($0.001<p<0.01$, Dunnett's Test), suggesting that the lack of surface-associated A-band and B-band polysaccharide facilitates attachment in the *waaL* mutant but that the loss of Psl takes precedence over the LPS alteration in defining the *rmlC* attachment phenotype. The increase in attachment of the *waaL* strain is not due to an increase in Psl expression, as the *waaL* mutant produced Psl at a level comparable to that of PAO1.

To demonstrate the specificity of Psl biosynthetic enzymes for the L-isoform of rhamnose, an *rmd* mutant was evaluated for surface attachment and Psl production (Fig. 6). Rmd is a GDP-4-keto-6-deoxy-D-mannose reductase and performs the final step in conversion of GDP-D-Man into GDP-D-Rha, the substrate for A-band polysaccharide production (Maki *et al.*, 2002; Rocchetta *et al.*, 1998). Since GDP-D-Rha synthesis occurs downstream of GDP-D-Man synthesis, we predicted that deletion of *rmd* would result in a loss of only A-band LPS. The *rmd* mutant was not defective in attachment but in fact attached to a greater degree than wild type ($p<0.05$, Dunnett's Test). This is similar to the *waaL*-deficient strain and suggests that the loss of A-band LPS increases attachment, perhaps by alteration of the surface properties of the cell. Psl production in the *rmd* mutant was detectable by immunoblot, but *rmd* extracts reacted substantially weaker with α-Psl compared to wild type. Deletion of *rmd* may result in accumulation of GDP-D-Man that inhibits the phosphomannose isomerase (PMI) activity of PslB, resulting in a reduction in Psl (Lee *et al.*, 2008). This explanation, however, does not take into account the compensatory PMI function of WbpW (see discussion below, Fig. 7), an enzyme for which GDP-D-Man feedback inhibition has yet to be demonstrated. It is unlikely that α-Psl is cross-reactive with A-band LPS since WFPA800 produces A-band LPS at a level comparable to that of wild type (see Fig. 9A), but displays no detectable reactivity with α-Psl. The observed reactivity of extracts from the *rmd* but not the *rmlC* mutant with α-Psl confirms that Psl enzymes rely on the precursor sugar nucleotide dTDP-L-Rha in Psl production and cannot use GDP-D-Rha exclusively. The intermediate Psl phenotype of the *rmd* mutant, however, does not rule out a contribution by GDP-D-Rha.

### UDP-D-Glc is required for Psl synthesis

Continuing with the analysis of sugar precursors incorporated into the Psl structure, we predicted that interfering with UDP-D-Glc generation would likewise prevent synthesis of Psl and result in defective surface attachment characteristic of the Psl-null phenotype. In *P. aeruginosa*, *galU* encodes the UDP-D-Glc pyrophosphorylase which joins Glc-1-P to its nucleotide carrier in the final step of the UDP-D-Glc pathway (Rocchetta *et al.*, 1999). Similar to deletion of *rmlC*, interruption of *galU* results in truncation of the LPS outer core

preventing surface expression of both A-band and B-band LPS (Choudhury *et al.*, 2005). Unlike the *rmlC* mutant, attachment of which is somewhat greater than WFPA800 ($p<0.05$, Tukey's Test), the *galU* mutant displays a significant ($p<0.001$, Dunnett's Test) defect in surface attachment comparable to that of WFPA800 (Fig. 6). Given that the loss of surface-associated A-band LPS appears to increase surface attachment, as in *rmlC*, *rmd*, and *waaL* mutants, resolving the lack of such an increase in the *galU* mutant will require further investigation. Immunoblotting extracts from the *galU* mutant revealed a complete loss of Psl as seen in the *rmlC*-deficient strain, confirming that in addition to dTDP-L-Rha, UDP-D-Glc is essential for Psl production. When compared to the *waaL* mutant lacking both A- and B-band LPS on the surface, the attachment phenotype of the *galU* mutant, similar to the *rmlC* strain, is dominated by the loss of Psl and not the loss of surface-associated A- and B-band LPS.

### WbpW allows for Psl production in a *pslB* mutant

The *pslM*, *pslN*, and *pslO* gene products have no homologs in *P. aeruginosa* and do not appear to have annotated functions associated with synthesis of a polysaccharide (Friedman and Kolter, 2004b; Jackson *et al.*, 2004; Stover *et al.*, 2000). PslB, however, is a paralog of WbpW and AlgA, being 60% identical at the amino acid level with WbpW (Jackson *et al.*, 2004; Rocchetta *et al.*, 1998). WbpW and AlgA have been shown to be bifunctional enzymes with PMI and GDP-D-Man pyrophosphorylase (GMP) activities and function in the A-band LPS and alginate pathways, respectively (Rocchetta *et al.*, 1998; Shinabarger *et al.*, 1991). It has been recently reported that PslB also possesses both PMI and GMP activities as predicted by homology to WbpW and AlgA (Lee *et al.*, 2008). In fact, prior to the *psl* nomenclature, an open reading frame designated *orf488* (*pslB*) was identified as coding for a putative PMI/GMP, and was positioned between two other *orf*s (*pslA* and *pslC*) collectively implicated in the synthesis of a polysaccharide containing D-Man, D-Glc, and L-Rha (Rocchetta *et al.*, 1998). In that same report, A-band LPS was produced at a low level in a *wbpW algA* double mutant, suggesting that ORF488/PslB was able to partially compensate for the loss of PMI/GMP activity in the synthesis of A-band LPS (Rocchetta *et al.*, 1998); however, this was not directly tested. Since PslB appears to be functional in the A-band LPS pathway, we hypothesized that WbpW compensates for PslB to allow for the production of GDP-D-Man and Psl in the *pslB* mutant. To test this we created an in-frame, non-polar *wbpW* deletion in the *pslB* background. A single *wbpW* mutant was also created to confirm that PslB is indeed functional in Psl synthesis. We did not delete *algA* in this study because the *algD* promoter responsible for transcription of *algA* is not significantly activated in nonmucoid strains, resulting in no detectable alginate (Wozniak and Ohman, 1994; Wozniak *et al.*, 2003).

Solid surface attachment for the *pslB wbpW* mutant was assessed, and polysaccharide extracts were used to quantify Psl production by immunoblot and ELISA (Fig. 7). Crystal violet staining revealed a significant ($p<0.001$) defect in attachment for the *pslB wbpW* mutant similar to that seen in the *psl* promoter deletion strain WFPA800 (Fig. 7A). The *wbpW* mutant exhibited a reduction in attachment ($p<0.001$) compared to wild type, yet still attached at approximately 80% of wild type. Immunoblot analysis of the *pslB wbpW* mutant

showed no detectable Psl, while the *wbpW* mutant produced Psl at a level similar to that of wild type (Fig. 7A).

To directly visualize attachment of the *pslB wbpW* mutant, we allowed mid-log cells to attach to vertically oriented glass coverslips for 4 h, then analyzed early biofilm formation at the air-liquid interface by scanning electron microscopy (Parise *et al.*, 2007). Wild type cells attached in a well-defined zone at the air-liquid interface, and upon higher magnification appeared tightly clustered and in contact with the glass along the long axes of the cells (Fig. 8A). In agreement with what is observed in the microtiter dish attachment assay, attachment of WFPA800 was greatly reduced compared to wild type; attaching only in isolated clusters of a few dozen cells each (Fig. 8B). The *pslB wbpW* double mutant attached similarly to WFPA800, confirming the attachment defect observed in the microtiter plate assay (Fig. 8E). The *wbpW* mutant displayed a well-defined line at the air-liquid interface similar to wild type, but had a web-like appearance in the submerged region of the coverslip (Fig. 8D). This may be related to the altered A-band phenotype (see Fig. 9A). Lastly, the *pslB* mutant showed abundant attachment both at the air-liquid interface and submerged regions of the coverslip (Fig. 8C). However, several of the *pslB* mutant cells were attached at the pole, in contrast to wild type or the other mutants (Fig. 8C). The cause of this altered attachment phenotype is not yet understood and will require further investigation of the surface properties of *pslB*-deficient cells compared to wild type and *wbpW* mutant cells.

An ELISA quantifying Psl production by these same strains revealed a complete loss of Psl in extracts from the *pslB wbpW* double mutant but no significant decrease for extracts derived from the *wbpW* mutant (Fig. 7B). Together, the attachment, immunoblot, and ELISA data confirm that, in a *pslB* mutant, WbpW is the PMI/GMP responsible for generating the GDP-D-Man essential in the production of Psl. The lack of a Psl phenotype in the *wbpW* mutant demonstrates that PslB does not require WbpW for Psl synthesis and is capable of functioning as a PMI/GMP, in agreement with recently published PslB enzymatic data (Lee *et al.*, 2008).

### PslB is the PMI/GMP that promotes A-band LPS production in a *wbpW* mutant

In a previous study, it was proposed that ORF488 (PslB) encoded a PMI/GMP responsible for the low level of A-band LPS observed in a *wbpW algA* mutant; however, *pslB* was not deleted in that study and therefore its role in A-band LPS synthesis could not be confirmed (Rocchetta *et al.*, 1998). The *pslB wbpW* double mutant generated in this study provides a means of addressing this unresolved question, namely, that PslB can serve as the PMI/GMP in the A-band LPS pathway much as WbpW can function as the PMI/GMP in the Psl pathway. A western blot analysis of A-band LPS using the A-band-specific monoclonal antibody N1F10 (Lam *et al.*, 1989) in *pslB*, *wbpW*, and *pslB wbpW* mutants was performed (Fig. 9). A-band LPS production in the *pslB* mutant and WFPA800 was similar to wild type, suggesting that no *psl* genes are needed for A-band synthesis and more specifically that WbpW functions as a PMI/GMP without PslB (Fig. 9A). Compared with the wild type strain, WFPA800, and the *pslB* mutant, the *wbpW* mutant produced reduced, but detectable A-band LPS in a faster migrating cluster of bands (Fig. 9A). A-band production in this mutant is presumably due to the PMI/GMP activity of PslB. In contrast to the other strains,

the *pslB wbpW* double mutant failed to produce detectable A-band polysaccharide (Fig. 9A), indicating that A-band LPS synthesis requires the redundant PMI/GMP activity of either PslB or WbpW to generate product.

The unexpected faster migration of N1F10-reactive bands in the *wbpW* mutant may be due to PslB functioning in an atypical pathway for a Psl enzyme, resulting in a shorter A-band polymer, but this explanation lacks a molecular basis since generation of GDP-D-Man by PslB occurs upstream of A-band assembly and should not interfere with this process. Although in-frame mutagenesis was performed, it is possible that deletion of *wbpW* had a polar effect on *wzm* and/or *wzt*, which are directly downstream of *wbpW* and encode the ABC transporter responsible for transport of A-band to the periplasm for attachment to the LPS core (Rocchetta and Lam, 1997). Deleting either of these genes results in A-band polysaccharide remaining in the cytoplasm attached to the lipid carrier Und-P, which runs slightly faster on a PAGE gel similar to what was seen in the *wbpW* mutant (Rocchetta and Lam, 1997). To address this, samples were prepared using the hot aqueous phenol method that results in cleavage of the highly labile A-band-Und-P linkage, preventing detection by western blotting (Rocchetta and Lam, 1997). Both A-band and B-band LPS were detectable for all strains except the *pslB wbpW* double mutant, indicating that the faster migrating bands in the *wbpW* mutant are not due to lipid linkage, but to another cause that remains to be determined (data not shown). The lack of A-band in the double mutant, however, indicates that in spite of possible polar effects on *wzm* and/or *wzt*, *wbpW* was indeed deleted and is not able to contribute to GDP-D-Man synthesis. As a control B-band LPS was analyzed by Western blot using the B-band-specific monoclonal antibody MF15-4 (Lam *et al.*, 1987). There were no differences in B-band LPS between the strains shown in Fig. 9A, confirming that neither WbpW nor PslB is involved in production of the sero-specific O-antigen (Fig. 9B).

## Conclusions and perspectives

In this study we have demonstrated that eleven of the fifteen *psl* genes, *pslACDEFGHIJKL*, are required for Psl synthesis and solid surface attachment. Prior to this work the structure of the Psl polysaccharide, while elucidated biochemically over two decades ago, had not been firmly linked to the *psl* operon. Here we show that the structure of Psl from cell-associated and growth medium fractions contains D-Man, D-Glc, and L-Rha in a pentasaccharide repeating unit distinct from other known polysaccharide moieties. Data presented in this study reveal a role for the sugar nucleotide precursors GDP-D-Man, UDP-D-Glc, and dTDP-L-Rha, all with previously identified functions in polysaccharide synthesis, in Psl polysaccharide production. Following up on the lack of a Psl phenotype in the *pslB* mutant, we have shown that the overlapping functions of PslB and WbpW permit Psl synthesis in a *pslB* mutant and A-band LPS synthesis in a *wbpW* mutant. The use of common precursors and similarly functioning enzymes in generating multiple polysaccharides demonstrates metabolic efficiency and contributes to the characteristic adaptability of *P. aeruginosa* as an opportunistic pathogen. For this overlap to be productive, however, it is important that products from all required pathways be expressed under the same conditions. Overlap among polysaccharide synthesis pathways is likewise apparent in other bacterial pathogens. In *E. coli* O9:K30, the O-antigen GMP RfbM produces sufficient GDP-Man for both O-

antigen and capsular polysaccharide production (Jayaratne *et al.*, 1994). The sugar nucleotide UDP-GlcNAc and its derivatives are also commonly shared among surface polysaccharides; PGA, peptidoglycan, and LPS in *E. coli* (Wang *et al.*, 2004), and LOS, capsule, and Pgl heptasaccharide in *Campylobacter jejuni* (Bernatchez *et al.*, 2005). A recent report identified redundant paralogs, at least one of which having a putative function in an LPS pathway, at both the initiating glycosyltransferase and polymerase steps in synthesis of the *Caulobacter crescentus* holdfast polysaccharide (Toh *et al.*, 2008). Although our understanding of the structure of Psl and the contribution of individual *psl* genes to Psl production has been extended by this study, much remains unknown about the functions of essential Psl proteins, regulation of the polysaccharide, and bacterial-host interactions mediated by Psl. It is also unclear how the Psl pentasaccharide repeating unit assembles into a biofilm matrix material. Future studies requiring biochemical, genetic, and immunological approaches will be necessary to fully understand the larger role of Psl in *P. aeruginosa* biology and pathogenesis.

## Experimental Procedures

### Strains and growth conditions

*Escherichia coli* strains were grown in Luria Bertani (LB; 10 g/L tryptone, 5 g/L yeast extract, 5 g/L NaCl) broth, and *P. aeruginosa* were routinely grown in LB or LB without NaCl (LBNS) at 37°C. Solid media with (LA) or without (LANS) NaCl were prepared with the addition of 1.5% agar. Sucrose was added at 5% for counterselection experiments. Antibiotics were used at the following concentrations: gentamicin (Gen) 15 and 100 μg/mL; ampicillin (Amp) 100 μg/mL; carbenicillin (Crb) 300 μg/mL; irgasan (Irg) 25 μg/mL. *E. coli* JM109 was used for cloning and SM10 for biparental mating with *P. aeruginosa*. Strains used in this study are presented in Table 1, and all plasmids and oligonucleotides are shown in Tables S1 and S2. Addition of L-arabinose at 2.0% was used for induction of Psl expression in WFPA801. For structural studies, *P. aeruginosa* were grown statically in 140–mm diameter Petri dishes in humidified chambers at 37°C for 24 hrs in M63 minimal medium ($(NH_4)_2SO_4$, 2g/L; $KH_2PO_4$, 13.6 g/L; $FeCl_3$, 0.5 mg/L); pH 7; supplemented with 0.5% Casaminoacids (Difco), 1 mM $MgCl_2$, and 0.2% glucose (Vasseur *et al.*, 2007). For growth of the *psl*-inducible WFPA801, medium was additionally supplemented with 0.4% L-arabinose (Acros Organic).

### Preparation of Psl for structural analysis

*P. aeruginosa* strains PAO1, WFPA801, and WFPA800 were grown statically in 140–mm diameter Petri dishes in humidified chambers at 37°C as outlined above. The transparent gelatinous material loosely attached to the bottom of the Petri dishes was collected together with the cells and growth medium. Cells and cell-associated matrix material were separated from the viscous growth media by centrifugation (6000 × *g*, 4°C, 30 min.). The pellet was suspended in 0.9% NaCl and the cell-surface-associated polymers were detached by mild sonication (IKA Labotecknik sonicator, 3 × 30 sec, 50% cycle, intensity 0.5). The pellet was removed by centrifugation and treated with a fresh portion of saline; this procedure was repeated twice more to give crude cell-associated matrix extract.

This extract and the growth media were further treated in the same way. TCA was added to a final concentration of 5% (wt/vol) in order to precipitate extracellular DNA and proteins. After centrifugation (10000 × *g*, 10 min.) the clear supernatant was extensively dialyzed and lyophilized. The residue was resuspended in water, the insoluble material removed by centrifugation (10000 × *g*, 10 min.), and the supernatant deproteinated by extraction with phenol (2×) and phenol-chloroform. The obtained crude carbohydrate extract was fractionated on a Sepahdex G-50 column.

Alternatively, WFPA801 and WFPA800 were grown in LBNS (0.5 L) with addition of 2% L-arabinose. Biomass was collected by centrifugation, re-suspended in 0.9% NaCl, vortexed, and pelleted. From the supernatant, extracellular DNA was removed by precipitation with 25% ethanol and 0.1 M $CaCl_2$. The supernatant was dialyzed, lyophilized, resuspended in water, and treated with proteinase K (final concentration 0.5 mg/mL) for 60 min at 60°C, followed by proteinase K inactivation for 30 min at 80°C. This crude polysaccharide extract was fractionated on a Sephadex G-50 column and carbohydrate-containing fractions were screened by Western immunoblotting.

## Analytical methods

*Methylation analysis* was carried out by the Ciucanu and Kerek method after reduction of polysaccharides with $NaBH_4$ (Ciucanu and Kerek, 1984).

**Gas-liquid chromatography—**Monosaccharides were identified by GLC on a Shimatzu GC-14 gas chromatograph equipped with flame ionization detector and Zebron ZB-5 capillary column (30 m × 0.25 mm), with hydrogen as carrier gas, using a temperature gradient 170°C (3 min.), 260°C at 5°C/min. Prior to analysis, polysaccharides were hydrolyzed with 4 M TFA (110°C, 3 h) and converted to alditol acetates by conventional methods.

**Gel-permeation chromatography—**Gel-permeation chromatography was carried out on a Sephadex G-50 column (1.6 × 95 cm; Pharmacia), irrigated with water. Fractions (5 mL) were assayed colorimetrically for aldose (Dubois, 1956). Dextrans with average molecular masses 1000, 5, and 1 KDa (Fluka) were used as MW markers.

**NMR spectroscopy—**Two-dimensional $^{1}H$ and $^{13}C$ NMR spectra were recorded using a Varian Inova 500 MHz and 400 MHz spectrometers for samples in $D_2O$ solutions at 25°C with acetone internal reference (2.23 ppm for $^{1}H$ and 31.5 ppm for $^{13}C$) using standard pulse sequences DQCOSY, TOCSY (mixing time 120 ms), NOESY (mixing time 400 ms), HSQC and HMBC (100 ms long range transfer delay).

## Manipulations and mutagenesis of *P. aeruginosa*

In-frame, non-polar deletions were made in each *psl* gene and *wbpW* using overlap extension PCR. *Eco*RI and *Hin*dIII cut sites were engineered into the outer pair of primers for cloning, except for *pslM* and *pslN* for which *Bam*HI was used in place of *Hin*dIII. Amplicons containing each deletion were digested with *Eco*RI and *Hin*dIII or *Bam*HI and cloned into pEX18Gm for *psl* genes or pEX18Ap for *wbpW*. Integrants in *P. aeruginosa*

were selected with Gen 100/Irg 25 for pEX18Gm or Crb 300/Irg 25 for pEX18Ap. Counterselection with sucrose was performed, and clones were confirmed by Gen 100 or Crb 300 sensitivity for pEX18Gm and pEX18Ap, respectively. Deletions were verified by sequencing of PCR amplicons, as well as complementation *in trans* for the *psl* mutants displaying a Psl-null phenotype.

### Generation of Psl antiserum

WFPA801 was grown on cellophane over LANS + 2% arabinose at 37°C overnight. Biomass was removed and resuspended in 250mL of 0.9% NaCl, vortexed and pelleted. The supernatant was precipitated with 95% ethanol at 4°C overnight and washed twice with 100% ethanol. The subsequent pellet was lyophilized and used for antisera generation by New England Peptide. New Zealand white rabbits were immunized with 400 μg of the crude Psl material followed by three subsequent boosts of 200 μg each. Serum from the final bleed was used for subsequent adsorptions. For adsorptions, WFPA800 cells were cultured on LANS plates, removed with LBNS, and pelleted. Intact bacteria ($\sim 10^5$ CFU) were resuspended in 5 mL final bleed serum and incubated with rocking at 4°C for 1 h. Cells were pelleted and supernatant was adsorbed repeatedly with fresh cells (total of four rounds). Antiserum enriched against Psl (α-Psl) was filtered through a 0.22 μm acrodisc filter, and aliquots were stored at -20°C.

### Western immunoblotting and ELISA of polysaccharide extracts

Crude polysaccharide extracts were obtained by resuspending approximately 10 OD equivalents (vol. [mL] = 10/culture $OD_{600}$) of overnight culture (~16 h) in 100 μL 0.5M EDTA and boiling 5 min. at 100°C (Parise *et al.*, 2007). The supernatant was collected and treated with proteinase K for 60 min. at 60°C (final concentration 0.5 mg/mL), followed by proteinase K inactivation for 30 min. at 80°C. Samples were stored at 4°C for immunoblotting and ELISA. For immunoblotting 1-5 μL of polysaccharide extract was spotted on a nitrocellulose membrane and allowed to air dry. The membrane was blocked with 10% skim milk in TBST (20 mM Tris, 137 mM NaCl, 0.1% Tween 20, pH 7.6) then probed with α-Psl (1:25000 in TBST) for 45 min. at 25°C with agitation. After washing, the secondary horseradish peroxidase-conjugated donkey anti-rabbit whole IgG (1:10000 in TBST, GE Healthcare) was applied and the blot incubated 45 min. at 25°C. The membrane was washed again and detected using SuperSignal West Dura Extended Duration Substrate per manufacturer's instructions (Pierce). Images were recorded using a Kodak Image Station 2000RT System and analyzed with Kodak Molecular Imaging Software.

In order to quantify Psl production an ELISA was modified from an existing protocol (Honko *et al.*, 2006). Flat-bottom 96-well MaxiSorp plates (Nunc) were coated in triplicate overnight at 4°C with 100 μL of a 1:100 dilution of the crude polysaccharide extracts also used for immunoblotting. Plates were washed 3× with wash buffer (PBS + 0.05% Tween 20) and blocked for 2 h at 25°C with 10% newborn calf serum in PBS. Plates were washed 3× and incubated with 100 μL α-Psl (1:25000 in PBS) for 2 h at 25°C. Following five washes, the secondary horseradish peroxidase-conjugated donkey anti-rabbit whole IgG (1:10000 in PBS, GE Healthcare) was applied and the plates incubated for 1 h at 25°C. The plates were washed 7× and 100 μL of 3,3′,5,5′-Tetramethylbenzidine (TMB, Sigma) substrate was

applied and incubated 30 min. at 25°C. To stop development 50 μL of a 2N solution of $H_2SO_4$ was added and the plates were read at 450 nm. Psl concentration was determined from absorbance values using a Psl standard curve then normalized to the optical density of cells used to make the polysaccharide extract. The Psl standard was the lyophilized extract used in antibody generation resuspended at a known concentration, typically 2 mg/mL, in pyrogen free distilled water.

### Microtiter dish attachment assay

Attachment of *P. aeruginosa* cells to an abiotic surface was evaluated by crystal violet staining essentially as described (Ma *et al.*, 2006). A volume of 100 μL of mid-log culture ($OD_{600}$ ~0.5) was added to the wells of a 96-well PVC microtiter plate (BD Falcon) and allowed to attach for 30 min. at 25°C. Nonattached cells were removed and the plate rinsed thoroughly with water. For staining, 100 μL of a 0.1% crystal violet solution was added to each well and the plate incubated for 30 min. at 25°C. After washing as above, the crystal violet bound to cells was solubilized in 200 μL of 95% ethanol for 30 min. at 25°C, then 100 μL of the solution was transferred to a new polystyrene microtiter plate to measure absorbance at 540 nm.

### LPS preparation and Western blot analysis

LPS was prepared by the proteinase K method (Hitchcock and Brown, 1983) from *P. aeruginosa* grown overnight on plates at 37°C. Cells (1 mL $OD_{600}$ ~0.5) were collected and treated with proteinase K overnight at 55°C. LPS was separated on a 12.5% SDS-PAGE gel, transferred to a BioTrace172 NT nitrocellulose membrane (Pall) and analyzed by Western immunoblotting as described previously (Rocchetta *et al.*, 1998). Mouse-derived monoclonal antibodies N1F10 (Lam *et al.*, 1989) and MF15-4 (Lam *et al.*, 1987) specific for A-band and B-band LPS, respectively, were used to probe membranes. Blots were developed using goat anti-mouse alkaline phosphatase-conjugated secondary antibody (Jackson ImmunoResearch) and BCIP/NBT (Sigma).

### Scanning electron microscopy

Biofilm formation was visualized essentially as described (Parise *et al.*, 2007). Cells grown to mid-log ($OD_{600}$ ~0.5) were allowed to attach 4 h at 25°C on vertically oriented 12 mm coverslips partially submerged in culture to create an air-liquid interface. Coverslips were gently rinsed in PBS, fixed with 2.5% glutaraldehyde for 1 h, and routinely processed for SEM. Cells were visualized using a Philips 515 SEM.

### Statistical calculations and image processing

Graphing and statistical analyses were performed using GraphPad Prism 5 (GraphPad Software, Inc.). Images were processed using Adobe Photoshop 7.0 (Adobe Systems, Inc.). Figures were assembled using Adobe Illustrator 10.0 (Adobe Systems, Inc.).

## Supplementary Material

Refer to Web version on PubMed Central for supplementary material.

## Acknowledgments

The authors wish to acknowledge Ken Grant and MicroMed for assistance with microscopy, Cynthia Ryder, Jordi Torrelles, John Gunn, and Elizabeth Waligora for scientific and manuscript advice. The *galU* mutant strain was kindly provided by Bob Hancock and Irith Wiegand of the University of British Columbia. This work was supported by Public Health Service grants AI061396 and HL058334 (D.J.W) and NRSA fellowship AI07870002 (M.S.B) and by an operating grant from the Canadian Cystic Fibrosis Foundation (J.S.L.). J.S.L. holds a Canadian Research Chair in Cystic Fibrosis and Microbial Glycobiology.

## References

Abeyrathne PD, Daniels C, Poon KK, Matewish MJ, Lam JS. Functional characterization of WaaL, a ligase associated with linking O-antigen polysaccharide to the core of Pseudomonas aeruginosa lipopolysaccharide. J Bacteriol. 2005; 187:3002–3012. [PubMed: 15838026]

Abeyrathne PD, Lam JS. WaaL of Pseudomonas aeruginosa utilizes ATP in in vitro ligation of O antigen onto lipid A-core. Mol Microbiol. 2007; 65:1345–1359. [PubMed: 17697256]

Bernatchez S, Szymanski CM, Ishiyama N, Li J, Jarrell HC, Lau PC, Berghuis AM, Young NM, Wakarchuk WW. A single bifunctional UDP-GlcNAc/Glc 4-epimerase supports the synthesis of three cell surface glycoconjugates in Campylobacter jejuni. J Biol Chem. 2005; 280:4792–4802. [PubMed: 15509570]

Branda SS, Vik S, Friedman L, Kolter R. Biofilms: the matrix revisited. Trends Microbiol. 2005; 13:20–26. [PubMed: 15639628]

Bystrova OV, Knirel YA, Lindner B, Kocharova NA, Kondakova AN, Zahringer U, Pier GB. Structures of the core oligosaccharide and O-units in the R- and SR-type lipopolysaccharides of reference strains of Pseudomonas aeruginosa O-serogroups. FEMS Immunol Med Microbiol. 2006; 46:85–99. [PubMed: 16420601]

Campisano A, Schroeder C, Schemionek M, Overhage J, Rehm BH. PslD is a secreted protein required for biofilm formation by Pseudomonas aeruginosa. Appl Environ Microbiol. 2006; 72:3066–3068. [PubMed: 16598021]

Choudhury B, Carlson RW, Goldberg JB. The structure of the lipopolysaccharide from a galU mutant of Pseudomonas aeruginosa serogroup-O11. Carbohydr Res. 2005; 340:2761–2772. [PubMed: 16229827]

Ciucanu I, Kerek F. A simple and rapid method for the permethylation of carbohydrates. Carbohyrdate Research. 1984; 131:209–217.

Dong C, Major LL, Srikannathasan V, Errey JC, Giraud MF, Lam JS, Graninger M, Messner P, McNeil MR, Field RA, Whitfield C, Naismith JH. RmlC, a C3′ and C5′ carbohydrate epimerase, appears to operate via an intermediate with an unusual twist boat conformation. J Mol Biol. 2007; 365:146–159. [PubMed: 17046787]

Driscoll JA, Brody SL, Kollef MH. The epidemiology, pathogenesis and treatment of Pseudomonas aeruginosa infections. Drugs. 2007; 67:351–368. [PubMed: 17335295]

Dubois M. Colorimetric methods for determination of sugars and related substances. Anal Biochem. 1956; 28:350–356.

Friedman L, Kolter R. Genes involved in matrix formation in Pseudomonas aeruginosa PA14 biofilms. Mol Microbiol. 2004a; 51:675–690. [PubMed: 14731271]

Friedman L, Kolter R. Two genetic loci produce distinct carbohydrate-rich structural components of the Pseudomonas aeruginosa biofilm matrix. J Bacteriol. 2004b; 186:4457–4465. [PubMed: 15231777]

Goodman AL, Kulasekara B, Rietsch A, Boyd D, Smith RS, Lory S. A signaling network reciprocally regulates genes associated with acute infection and chronic persistence in Pseudomonas aeruginosa. Dev Cell. 2004; 7:745–754. [PubMed: 15525535]

Govan JR, Deretic V. Microbial pathogenesis in cystic fibrosis: mucoid Pseudomonas aeruginosa and Burkholderia cepacia. Microbiol Rev. 1996; 60:539–574. [PubMed: 8840786]

Hancock RE, Mutharia LM, Chan L, Darveau RP, Speert DP, Pier GB. Pseudomonas aeruginosa isolates from patients with cystic fibrosis: a class of serum-sensitive, nontypable strains deficient in lipopolysaccharide O side chains. Infect Immun. 1983; 42:170–177. [PubMed: 6413410]

Hickman JW, Tifrea DF, Harwood CS. A chemosensory system that regulates biofilm formation through modulation of cyclic diguanylate levels. Proc Natl Acad Sci U S A. 2005; 102:14422–14427. [PubMed: 16186483]

Hitchcock PJ, Brown TM. Morphological heterogeneity among Salmonella lipopolysaccharide chemotypes in silver-stained polyacrylamide gels. J Bacteriol. 1983; 154:269–277. [PubMed: 6187729]

Holloway BW. Genetic recombination in Pseudomonas aeruginosa. J Gen Microbiol. 1955; 13:572–581. [PubMed: 13278508]

Honko AN, Sriranganathan N, Lees CJ, Mizel SB. Flagellin is an effective adjuvant for immunization against lethal respiratory challenge with Yersinia pestis. Infect Immun. 2006; 74:1113–1120. [PubMed: 16428759]

Jackson KD, Starkey M, Kremer S, Parsek MR, Wozniak DJ. Identification of psl, a locus encoding a potential exopolysaccharide that is essential for Pseudomonas aeruginosa PAO1 biofilm formation. J Bacteriol. 2004; 186:4466–4475. [PubMed: 15231778]

Jayaratne P, Bronner D, MacLachlan PR, Dodgson C, Kido N, Whitfield C. Cloning and analysis of duplicated rfbM and rfbK genes involved in the formation of GDP-mannose in Escherichia coli O9:K30 and participation of rfb genes in the synthesis of the group I K30 capsular polysaccharide. J Bacteriol. 1994; 176:3126–3139. [PubMed: 7515042]

Kocharova NA, Knirel YA, Shashkov AS, Kochetkov NK, Pier GB. Structure of an extracellular cross-reactive polysaccharide from Pseudomonas aeruginosa immunotype 4. J Biol Chem. 1988; 263:11291–11295. [PubMed: 3136157]

Komarova BS, Tsvetkov YE, Pier GB, Nifantiev NE. First Synthesis of Pentasaccharide Glycoform I of the Outer Core Region of the Pseudomonas aeruginosa Lipopolysaccharide. J Org Chem. 2008

Lam JS, MacDonald LA, Lam MY, Duchesne LG, Southam GG. Production and characterization of monoclonal antibodies against serotype strains of Pseudomonas aeruginosa. Infect Immun. 1987; 55:1051–1057. [PubMed: 2437030]

Lam MY, McGroarty EJ, Kropinski AM, MacDonald LA, Pedersen SS, Hoiby N, Lam JS. Occurrence of a common lipopolysaccharide antigen in standard and clinical strains of Pseudomonas aeruginosa. J Clin Microbiol. 1989; 27:962–967. [PubMed: 2501356]

Lee HJ, Chang HY, Venkatesan N, Peng HL. Identification of amino acid residues important for the phosphomannose isomerase activity of PslB in Pseudomonas aeruginosa PAO1. FEBS Lett. 2008; 582:3479–3483. [PubMed: 18801364]

Ma L, Jackson KD, Landry RM, Parsek MR, Wozniak DJ. Analysis of Pseudomonas aeruginosa conditional psl variants reveals roles for the psl polysaccharide in adhesion and maintaining biofilm structure postattachment. J Bacteriol. 2006; 188:8213–8221. [PubMed: 16980452]

Ma L, Lu H, Sprinkle A, Parsek MR, Wozniak DJ. Pseudomonas aeruginosa Psl is a galactose- and mannose-rich exopolysaccharide. J Bacteriol. 2007; 189:8353–8356. [PubMed: 17631634]

Ma L, Conover M, Lu H, Parsek MR, Bayles K, Wozniak DJ. Assembly and development of the Pseudomonas aeruginosa biofilm matrix. PLoS Pathog. 2009; 5:e1000354. [PubMed: 19325879]

Maki M, Jarvinen N, Rabina J, Roos C, Maaheimo H, Renkonen R. Functional expression of Pseudomonas aeruginosa GDP-4-keto-6-deoxy-d-mannose reductase which synthesizes GDP-rhamnose. Eur J Biochem. 2002; 269:593–601. [PubMed: 11856318]

Matsukawa M, Greenberg EP. Putative exopolysaccharide synthesis genes influence Pseudomonas aeruginosa biofilm development. J Bacteriol. 2004; 186:4449–4456. [PubMed: 15231776]

Parise G, Mishra M, Itoh Y, Romeo T, Deora R. Role of a putative polysaccharide locus in Bordetella biofilm development. J Bacteriol. 2007; 189:750–760. [PubMed: 17114249]

Parsek MR, Singh PK. Bacterial biofilms: an emerging link to disease pathogenesis. Annu Rev Microbiol. 2003; 57:677–701. [PubMed: 14527295]

Poon KK, Westman EL, Vinogradov E, Jin S, Lam JS. Functional characterization of MigA and WapR: putative rhamnosyltransferases involved in outer core oligosaccharide biosynthesis of Pseudomonas aeruginosa. J Bacteriol. 2008; 190:1857–1865. [PubMed: 18178733]

Rahim R, Burrows LL, Monteiro MA, Perry MB, Lam JS. Involvement of the rml locus in core oligosaccharide and O polysaccharide assembly in Pseudomonas aeruginosa. Microbiology. 2000; 146(Pt 11):2803–2814. [PubMed: 11065359]

Ramsey DM, Wozniak DJ. Understanding the control of Pseudomonas aeruginosa alginate synthesis and the prospects for management of chronic infections in cystic fibrosis. Mol Microbiol. 2005; 56:309–322. [PubMed: 15813726]

Rivera M, Bryan LE, Hancock RE, McGroarty EJ. Heterogeneity of lipopolysaccharides from Pseudomonas aeruginosa: analysis of lipopolysaccharide chain length. J Bacteriol. 1988; 170:512–521. [PubMed: 3123455]

Rivera M, McGroarty EJ. Analysis of a common-antigen lipopolysaccharide from Pseudomonas aeruginosa. J Bacteriol. 1989; 171:2244–2248. [PubMed: 2495275]

Rocchetta HL, Lam JS. Identification and functional characterization of an ABC transport system involved in polysaccharide export of A-band lipopolysaccharide in Pseudomonas aeruginosa. J Bacteriol. 1997; 179:4713–4724. [PubMed: 9244257]

Rocchetta HL, Pacan JC, Lam JS. Synthesis of the A-band polysaccharide sugar d-rhamnose requires Rmd and WbpW: identification of multiple AlgA homologues, WbpW and ORF488, in Pseudomonas aeruginosa. Mol Microbiol. 1998; 29:1419–1434. [PubMed: 9781879]

Rocchetta HL, Burrows LL, Lam JS. Genetics of O-antigen biosynthesis in Pseudomonas aeruginosa. Microbiol Mol Biol Rev. 1999; 63:523–553. [PubMed: 10477307]

Ryder C, Byrd M, Wozniak DJ. Role of polysaccharides in Pseudomonas aeruginosa biofilm development. Curr Opin Microbiol. 2007; 10:644–648. [PubMed: 17981495]

Sadovskaya I, Brisson JR, Lam JS, Richards JC, Altman E. Structural elucidation of the lipopolysaccharide core regions of the wild-type strain PAO1 and O-chain-deficient mutant strains AK1401 and AK1012 from Pseudomonas aeruginosa serotype O5. Eur J Biochem. 1998; 255:673–684. [PubMed: 9738907]

Sadovskaya I, Brisson JR, Thibault P, Richards JC, Lam JS, Altman E. Structural characterization of the outer core and the O-chain linkage region of lipopolysaccharide from Pseudomonas aeruginosa serotype O5. Eur J Biochem. 2000; 267:1640–1650. [PubMed: 10712594]

Sadovskaya I, Vinogradov E, Li J, Jabbouri S. Structural elucidation of the extracellular and cell-wall teichoic acids of Staphylococcus epidermidis RP62A, a reference biofilm-positive strain. Carbohydr Res. 2004; 339:1467–1473. [PubMed: 15178389]

Samuel G, Reeves P. Biosynthesis of O-antigens: genes and pathways involved in nucleotide sugar precursor synthesis and O-antigen assembly. Carbohydr Res. 2003; 338:2503–2519. [PubMed: 14670712]

Shinabarger D, Berry A, May TB, Rothmel R, Fialho A, Chakrabarty AM. Purification and characterization of phosphomannose isomerase-guanosine diphospho-d-mannose pyrophosphorylase. A bifunctional enzyme in the alginate biosynthetic pathway of Pseudomonas aeruginosa. J Biol Chem. 1991; 266:2080–2088. [PubMed: 1846611]

Soberon-Chavez G, Lepine F, Deziel E. Production of rhamnolipids by Pseudomonas aeruginosa. Appl Microbiol Biotechnol. 2005; 68:718–725. [PubMed: 16160828]

Starkey M, Hickman JH, Ma L, Zhang N, De Long S, Hinz A, Palacios S, Manoil C, Kirisits MJ, Starner TD, Wozniak DJ, Harwood CS, Parsek MR. Pseudomonas aeruginosa rugose small-colony variants have adaptations that likely promote persistence in the cystic fibrosis lung. J Bacteriol. 2009; 191:3492–3503. [PubMed: 19329647]

Stewart PS, Costerton JW. Antibiotic resistance of bacteria in biofilms. Lancet. 2001; 358:135–138. [PubMed: 11463434]

Stover CK, Pham XQ, Erwin AL, Mizoguchi SD, Warrener P, Hickey MJ, Brinkman FS, Hufnagle WO, Kowalik DJ, Lagrou M, Garber RL, Goltry L, Tolentino E, Westbrock-Wadman S, Yuan Y, Brody LL, Coulter SN, Folger KR, Kas A, Larbig K, Lim R, Smith K, Spencer D, Wong GK, Wu Z, Paulsen IT, Reizer J, Saier MH, Hancock RE, Lory S, Olson MV. Complete genome sequence of Pseudomonas aeruginosa PA01, an opportunistic pathogen. Nature. 2000; 406:959–964. [PubMed: 10984043]

Toh E, Kurtz HD Jr, Brun YV. Characterization of the Caulobacter crescentus holdfast polysaccharide biosynthesis pathway reveals significant redundancy in the initiating glycosyltransferase and polymerase steps. J Bacteriol. 2008; 190:7219–7231. [PubMed: 18757530]

Vasseur P, Vallet-Gely I, Soscia C, Genin S, Filloux A. The pel genes of the Pseudomonas aeruginosa PAK strain are involved at early and late stages of biofilm formation. Microbiology. 2005; 151:985–997. [PubMed: 15758243]

Vasseur P, Soscia C, Voulhoux R, Filloux A. PelC is a Pseudomonas aeruginosa outer membrane lipoprotein of the OMA family of proteins involved in exopolysaccharide transport. Biochimie. 2007; 89:903–915. [PubMed: 17524545]

Vinogradov E, Sadovskaya I, Li J, Jabbouri S. Structural elucidation of the extracellular and cell-wall teichoic acids of Staphylococcus aureus MN8m, a biofilm forming strain. Carbohydr Res. 2006; 341:738–743. [PubMed: 16458275]

Wang X, Preston JF 3rd, Romeo T. The pgaABCD locus of Escherichia coli promotes the synthesis of a polysaccharide adhesin required for biofilm formation. J Bacteriol. 2004; 186:2724–2734. [PubMed: 15090514]

Whitfield C, Roberts IS. Structure, assembly and regulation of expression of capsules in Escherichia coli. Mol Microbiol. 1999; 31:1307–1319. [PubMed: 10200953]

Wozniak DJ, Ohman DE. Transcriptional analysis of the Pseudomonas aeruginosa genes algR, algB, and algD reveals a hierarchy of alginate gene expression which is modulated by algT. J Bacteriol. 1994; 176:6007–6014. [PubMed: 7928961]

Wozniak DJ, Wyckoff TJ, Starkey M, Keyser R, Azadi P, O′Toole GA, Parsek MR. Alginate is not a significant component of the extracellular polysaccharide matrix of PA14 and PAO1 Pseudomonas aeruginosa biofilms. Proc Natl Acad Sci U S A. 2003; 100:7907–7912. [PubMed: 12810959]

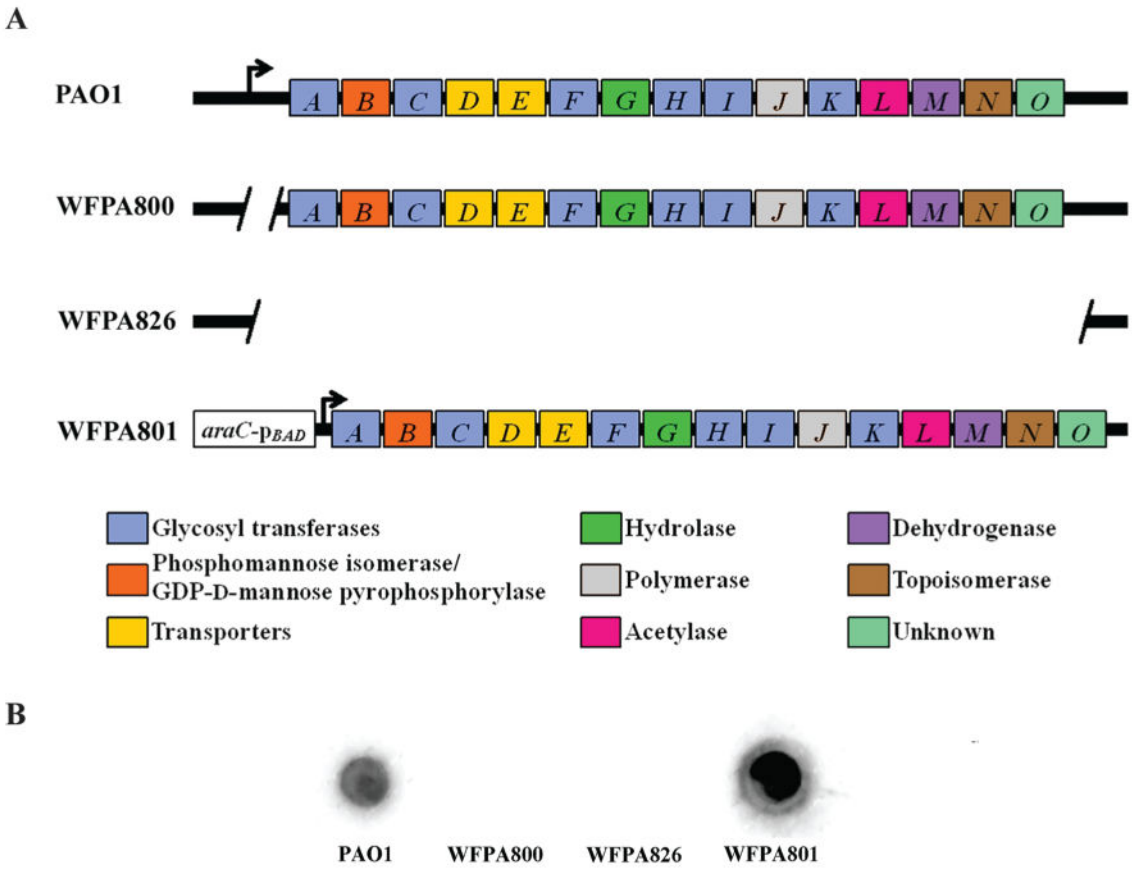


**Figure 1.**

Structure of the *psl* operon and confirmation of Psl-specific antisera.

A. Map of the *psl* operon in PAO1 and selected mutants used in this study. Genes *pslA-O* are shown in boxes (not to scale), with the color corresponding to the putative functions assigned to the gene products, shown in the lower panel. Functions were assigned using bioinformatics by three independent sources (Friedman and Kolter, 2004b; Jackson *et al.*, 2004; Stover *et al.*, 2000). Angled lines represent the extent of deleted sequence, and black arrows indicate transcriptional start sites (not to scale).

B. Crude polysaccharide extracts from PAO1, WFPA800, WFPA826, and WFPA801 were blotted on nitrocellulose, probed with α-Psl, and detected by chemiluminescence using a HRP-conjugated secondary antibody. Extract from WFPA801 was diluted 1:50 in order to remain within range of detection.

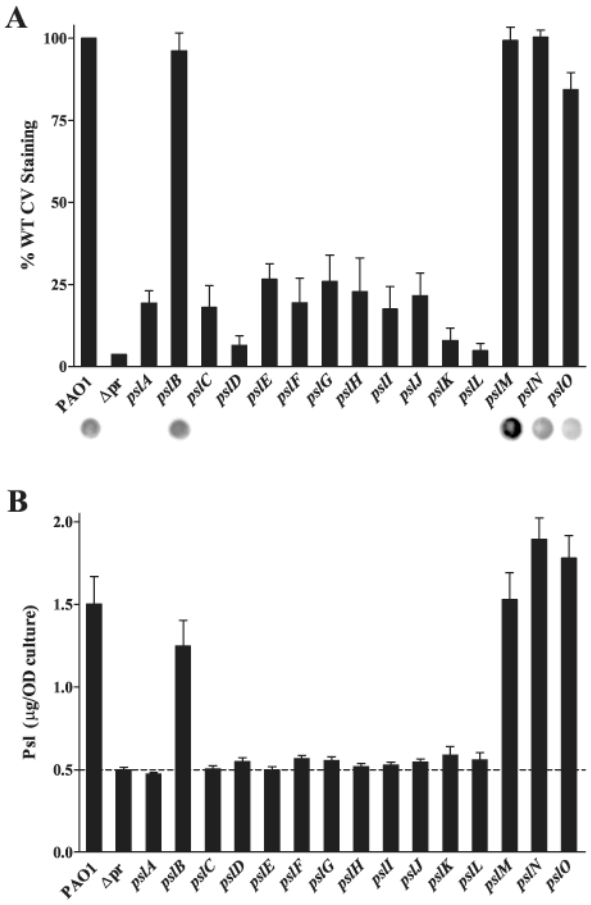


**Figure 2.**

Mutagenesis of *psl* genes reveals that *pslACDEFGHIJKL* are necessary for Psl synthesis and *P. aeruginosa* attachment.

A. Solid surface attachment of *psl* single mutants correlates with Psl production. Crystal violet staining, read at 540 nm, shown as a percentage of PAO1. The promoter deletion strain WFPA800 is notated as Δpr in both A and B. Values are mean ± SEM from two experiments each in triplicate. Psl production by α-Psl immunoblot is shown below each bar.

B. Psl is produced by eleven of fifteen *psl* single mutants. ELISA performed using plates coated with crude polysaccharide extracts and probed with α-Psl, read at 450 nm. Values are mean ± SEM from two experiments each in triplicate; dashed line shows background signal of extracts derived from the Δ*pr* strain, WFPA800. The mass of Psl is normalized to $OD_{600}$ equivalents used to generate the extracts.

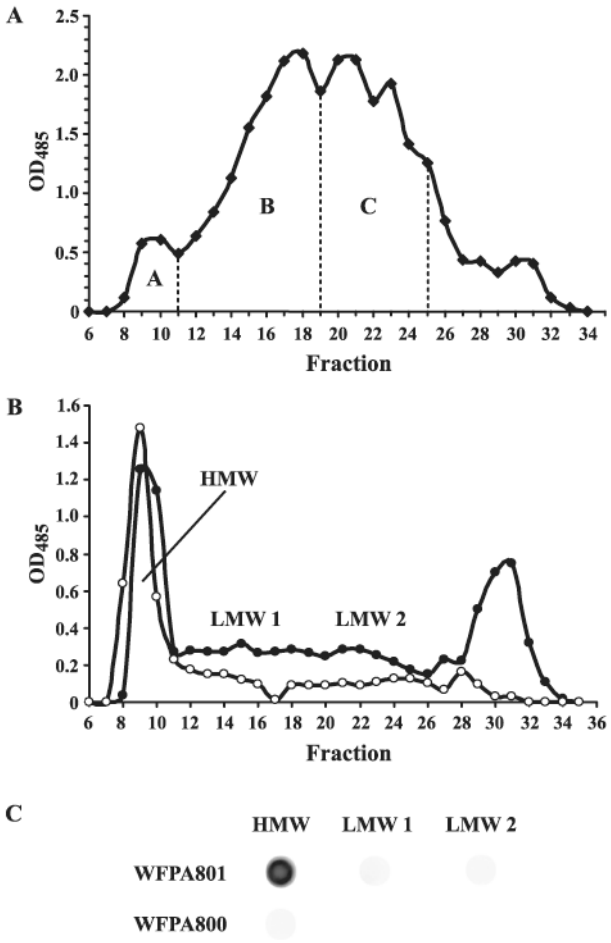


**Figure 3.**

Fractionation of carbohydrate extracts reveals a *psl*-dependent polysaccharide.

A. Typical elution profile of crude carbohydrate extract of the growth medium (1 L) of *P. aeruginosa psl*-inducible strain WFPA801 on a Sephadex G-50 column. Cells were grown in M63 medium (1 L) with addition of L-arabinose (0.4 %). Fractions A, B, and C are as indicated. Fractions B and C contain polysaccharide with ∼3-5 and ∼1-2 pentasaccharide repeating units, respectively. Fraction C was used for detailed NMR analysis.

B. Elution profile of crude carbohydrate extracts of the growth medium of *P. aeruginosa psl*-inducible strain WFPA801 (closed circles) and *psl* promoter deletion strain WFPA800 (open circles) on a Sephadex G-50 column. Cells were grown in 0.5 L LBNS with addition of 2.0% L-arabinose. A high MW fraction (HMW) and two low MW fractions (LMW 1 and LMW 2) are as indicated.

C. Antiserum reactivity with WFPA801 and WFPA800 cell-associated polysaccharide fractions from B screened by immunoblot analysis.

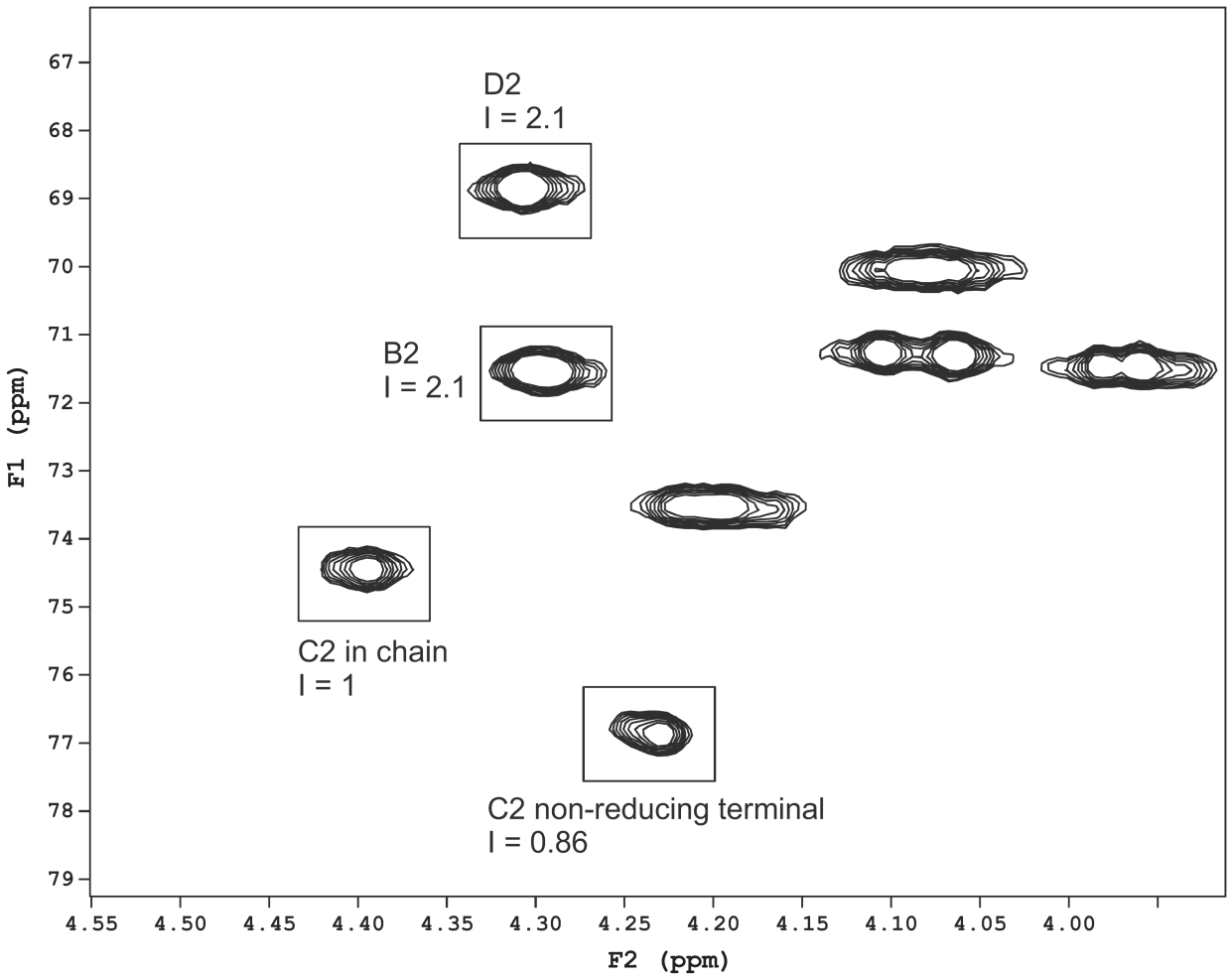


**Figure 4.**
Partial 2D HSQC spectrum of Psl and the integration data of signals, characteristic for a single pentasaccharide repeating unit (structure I) and its oligomers. I, integral value.

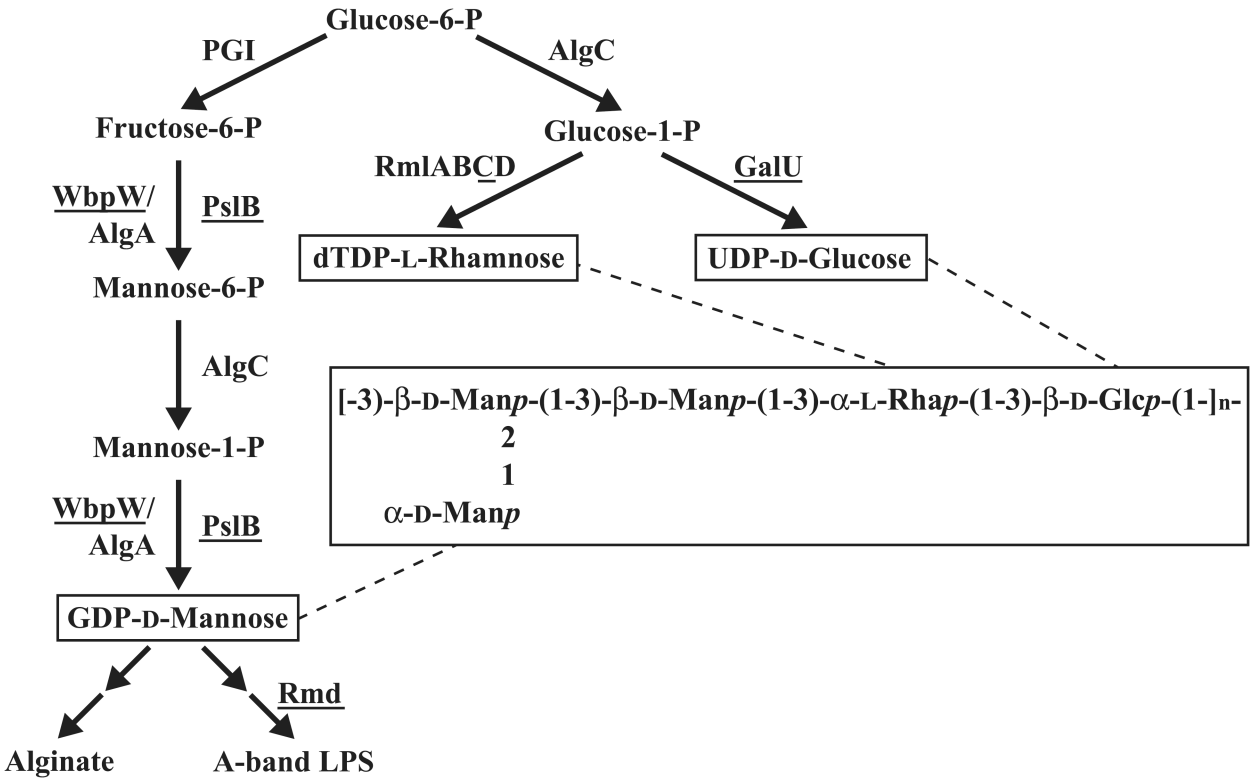


**Figure 5.**

Pathways involved in synthesis of Psl sugar nucleotide precursors.

Terminal steps of GDP-D-Man, UDP-D-Glc, and dTDP-L-Rha synthesis pathways shown. Sugar nucleotides are shown in boxes and enzymes deleted in this study are underlined. In the Psl repeating unit s`, larger box, *p* indicates the pyranosyl form of the monosaccharide residue. PGI, phosphoglucose isomerase.

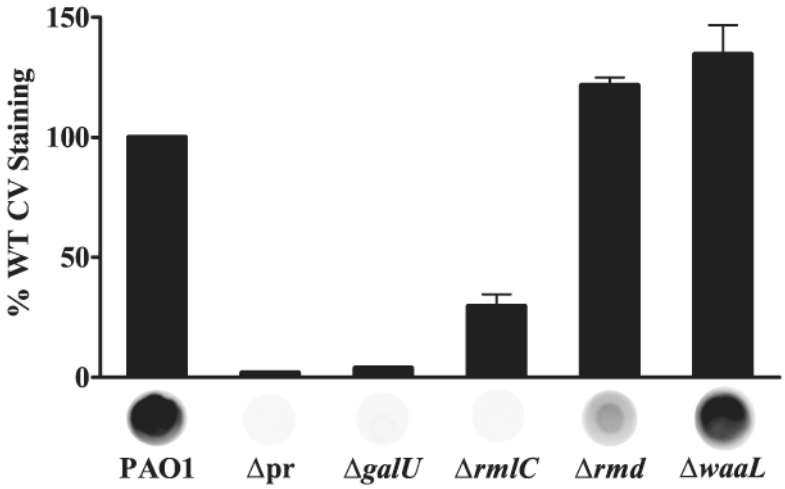


**Figure 6.**

dTDP-L-Rha and UDP-D-Glc are essential for Psl production.

Deletion of *rmlC* or *galU* results in defective surface attachment due to loss of Psl, while loss of *rmd* does not affect attachment despite a reduction in Psl. Crystal violet staining, read at 540 nm, shown as a percentage of PAO1. The promoter deletion strain WFPA800 is notated as Δpr. Values are mean ± SEM from two or three experiments. Psl production by α-Psl immunoblot shown below each bar.

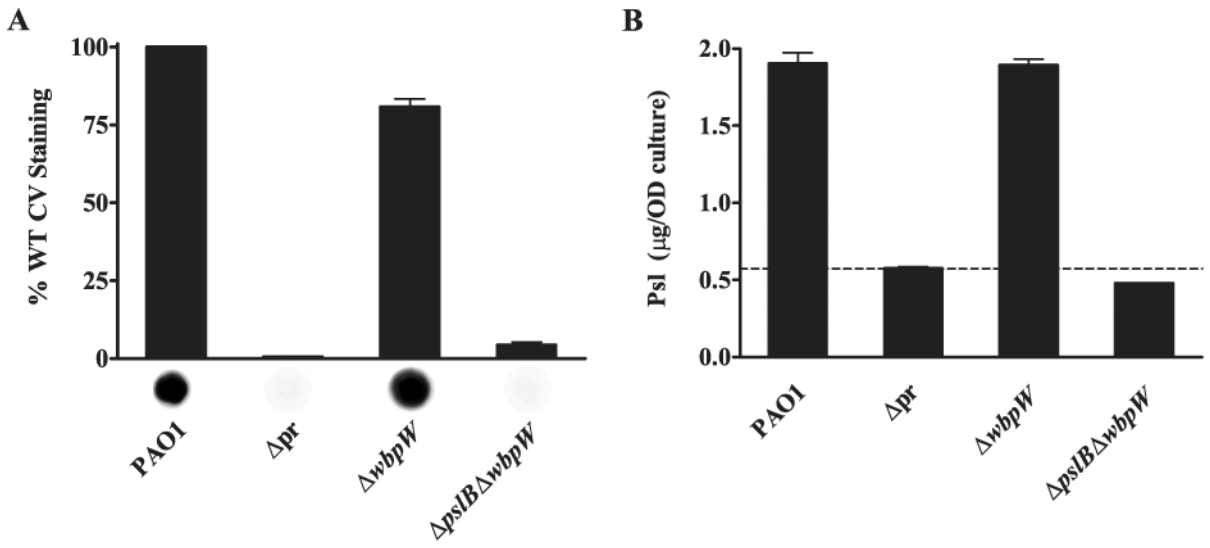


**Figure 7.**

WbpW is the PMI/GMP in Psl synthesis in the absence of PslB.

A. Deletion of *pslB* and *wbpW* results in an attachment defect and loss of Psl. Crystal violet staining, read at 540 nm, shown as a percentage of PAO1. The promoter deletion strain WFPA800 is notated as Δpr in both A and B. Values are mean ± SEM from three experiments. Psl production by α-Psl immunoblot shown below each bar.

B. Psl is produced by a *wbpW* mutant but not by a *pslB wbpW* double mutant. ELISA performed using plates coated with crude polysaccharide extracts and probed with α-Psl, read at 450 nm. Values are mean ± SEM from two experiments each in triplicate; dashed line shows background signal of extracts derived from the Δ*pr* strain, WFPA800. The mass of Psl is normalized to $OD_{600}$ equivalents used to generate the extracts.

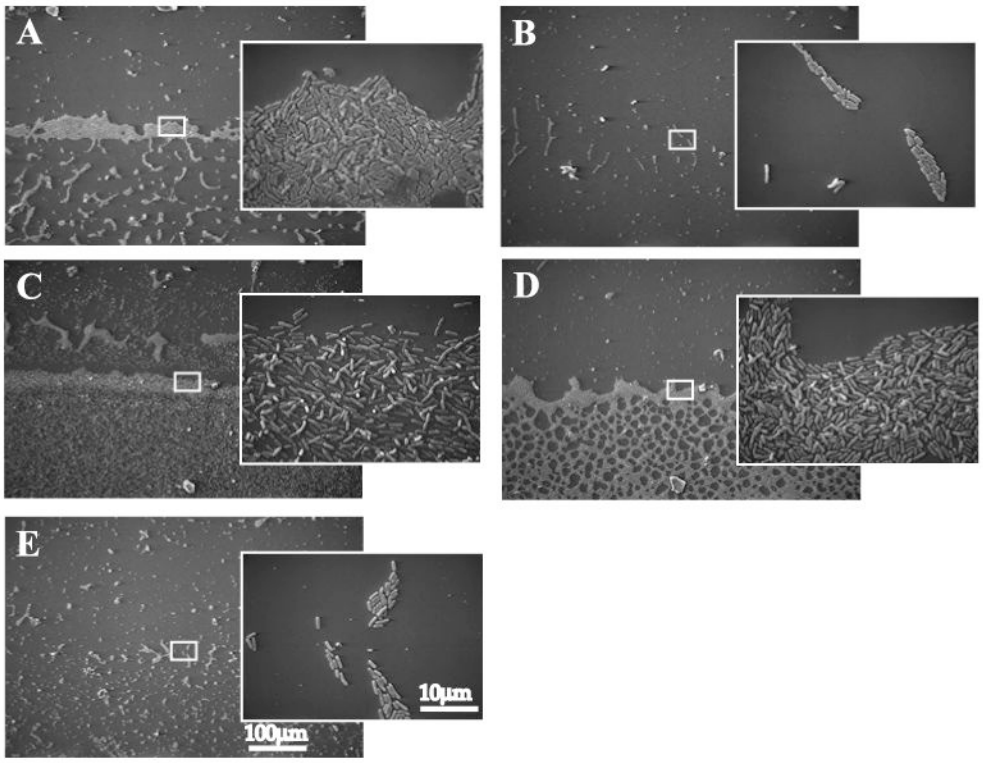


**Figure 8.**

Attachment phenotypes of *pslB* and *wbpW* single and double mutants.

Cells were allowed to attach to vertically oriented glass coverslips for 4 h, then fixed and visualized by SEM. A, PAO1; B, WFPA800; C, *pslB*; D, *wbpW*; E, *pslB wbpW*. Larger images taken at 170×, inset images taken at 2500×. White boxes indicate the magnified region of the air-liquid interface shown in inset.

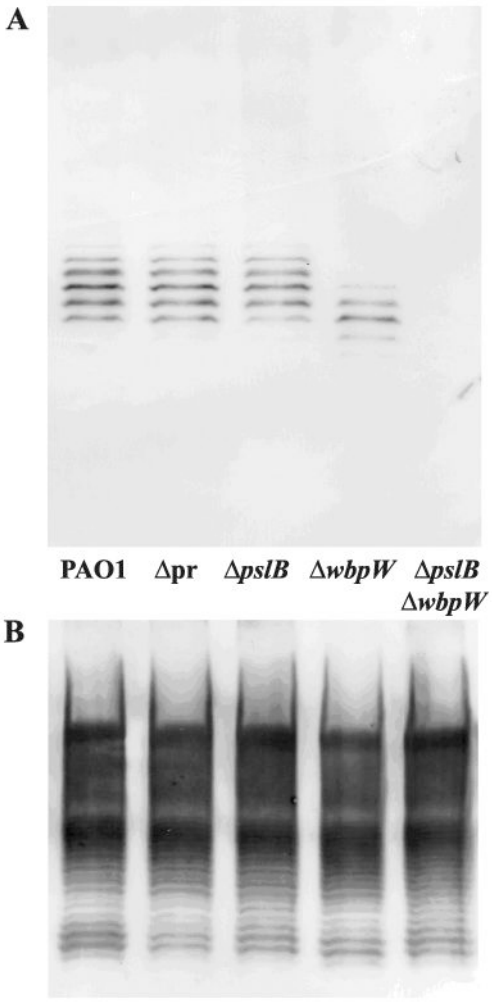


**Figure 9.**

PslB is the PMI/GMP in A-band LPS synthesis in the absence of WbpW.

A. A-band LPS is detectable in a *wbpW* mutant but not in a *pslB wbpW* double mutant. LPS was purified from *P. aeruginosa* grown on plates 12 h at 37°C. Western blot analysis of PAO1, WFPA800 (notated as Δpr), *pslB*, *wbpW*, and *pslB wbpW*, using the A-band-specific mAb N1F10.

B. B-band LPS is unaffected in mutant *P. aeruginosa* strains. Western blot analysis of strains from A, using the B-band-specific mAb MF15-4.

**Table 1**

Strains used in this study.

| Strain | Genotype | Source |
|---|---|---|
| PAO1 | Prototroph | (Holloway, 1955) |
| WFPA800 | *psl* promoter deletion | Ma, *et al.* (2006) |
| WFPA801 | *psl-araC*-$p_{BAD}$ promoter replacement | Ma, *et al.* (2006) |
| WFPA811 | In-frame *pslA* deletion | This work |
| WFPA812 | In-frame *pslB* deletion | This work |
| WFPA813 | In-frame *pslC* deletion | This work |
| WFPA814 | In-frame *pslD* deletion | This work |
| WFPA815 | In-frame *pslE* deletion | This work |
| WFPA816 | In-frame *pslF* deletion | This work |
| WFPA817 | In-frame *pslG* deletion | This work |
| WFPA818 | In-frame *pslH* deletion | Ma, *et al.* (2007) |
| WFPA819 | In-frame *pslI* deletion | Ma, *et al.* (2007) |
| WFPA820 | In-frame *pslJ* deletion | This work |
| WFPA821 | In-frame *pslK* deletion | This work |
| WFPA822 | In-frame *pslL* deletion | This work |
| WFPA823 | In-frame *pslM* deletion | This work |
| WFPA824 | In-frame *pslN* deletion | This work |
| WFPA825 | In-frame *pslO* deletion | This work |
| WFPA841 | In-frame *wbpW* deletion | This work |
| WFPA842 | In-frame *pslB*, *wbpW* deletion | This work |
| RML-ΔC | Non-polar interruption of *rmlC* by FRT sequences | Rahim, *et al.* (2000) |
| $R1_{O5}$ | *rmd*::$Gm^R$ in PAO1 | Rocchetta, *et al.* (1998) |
| PAO1waaL | *waaL*::$Gm^R$ in PAO1 | Abeyrathne, *et al.* (2005) |
| PAO1-Δ*galU* | *galU*::$Gm^R$ in PAO1 | R. E. Hancock Lab |

**Table 2**

NMR data. Polysaccharide spectra were recorded at 30°C in $D_2O$ with acetone standard.

| | | δ (ppm) | | | | | | |
|---|---|---|---|---|---|---|---|---|
| **Unit** | **Nucleus** | **H/C 1** | **H/C 2** | **H/C 3** | **H/C 4** | **H/C 5** | **H/C 6a** | **H/C 6b** |
| α-Man A | H | 5.38 | 4.06 | 3.97 | 3.70 | 4.20 | 3.79 | 3.89 |
| | C | 101.5 | 71.3 | 71.5 | 67.8 | 73.5 | 61.5 | |
| α -Man A′ | H | 5.21 | 4.10 | 3.97 | 3.70 | 4.20 | 3.79 | 3.89 |
| | C | 102.3 | 71.3 | 71.5 | 67.8 | 73.5 | 61.5 | |
| α -Rha B | H | 5.14 | 4.30 | 3.94 | 3.59 | 4.08 | 1.27 | |
| | C | 102.1 | 71.5 | 80.6 | 72.3 | 70.0 | 17.7 | |
| β-Man C | H | 4.87 | 4.39 | 4.00 | 3.75 | 3.44 | 3.79 | 3.89 |
| | C | 97.8 | 74.4 | 82.4 | 66.8 | 77.7 | 61.5 | |
| β-Man C′ | H | 4.88 | 4.23 | 3.80 | 3.63 | 3.41 | 3.79 | 3.89 |
| | C | 97.8 | 76.8 | 74.9 | 68.1 | 77.9 | 61.5 | |
| β-Man D | H | 4.88 | 4.31 | 3.90 | 3.66 | 3.40 | 3.79 | 3.89 |
| | C | 102.4 | 68.9 | 80.3 | 66.3 | 77.4 | 61.5 | |
| β-Glc E | H | 4.65 | 3.47 | 3.63 | 3.48 | 3.48 | 3.73 | 3.93 |
| | C | 101.6 | 74.9 | 83.8 | 69.4 | 77.2 | 62.1 | |
| α -Glc E′ | H | 5.20 | 3.63 | 3.80 | 3.48 | 3.47 | 3.72 | 3.90 |
| | C | 93.4 | 73.2 | 80.9 | 69.4 | 77.2 | 62.1 | |
| β-Glc E″ | H | 4.65 | 3.35 | 3.61 | 3.47 | 3.47 | 3.72 | 3.90 |
| | C | 96.9 | 75.9 | 83.4 | 69.4 | 77.2 | 62.1 | |